Catalysis
Science &
Technology

PAPER

View Article Online
View Journal

Cite this: DOI: 10.1039/c4cy01464b

# Bi-functional $NH_2$-MIL-101(Fe) for one-pot tandem photo-oxidation/Knoevenagel condensation between aromatic alcohols and active methylene compounds†

Dengke Wang and Zhaohui Li*

Received 8th November 2014,
Accepted 2nd December 2014

DOI: 10.1039/c4cy01464b

www.rsc.org/catalysis

Tandem reactions, which enable multistep reactions in one pot, offer enormous economical advantages. For the first time, this manuscript reported that $NH_2$-MIL-101(Fe), an earth abundant Fe-containing MOF material, can catalyze efficiently the one-pot reaction between aromatic alcohols and active methylene compounds *via* a tandem photo-oxidation/Knoevenagel condensation under visible light and at room temperature. $NH_2$-MIL-101(Fe) acts as a photocatalyst for the oxidation of aromatic alcohols to aldehydes as well as a base catalyst for Knoevenagel condensation between the as-formed aldehydes and the active methylene compounds. The comparison of the reactions over $NH_2$-MIL-101(Fe) and another two MOFs ($NH_2$-UiO-66(Zr) and $NH_2$-MIL-125(Ti)) reveals that the strength of the basic sites in the MOFs influences significantly the efficiency of the tandem reaction. This study highlights the great potential of MOFs as multifunctional photocatalysts for one-pot tandem reactions.

## Introduction

Tandem reactions, which enable multistep reactions in one pot, have attracted a great deal of attention since they avoid the isolation of intermediates and reduce the production of wastes, thus offering enormous economical advantages.[1] Multifunctional catalysts which contains different catalytically active sites in a site-isolation manner to maintain their independent function is usually required for an efficient one-pot tandem reaction. Currently most of the already reported one-pot tandem reactions involve homogeneous catalysts, which usually suffer from product contamination and limited recyclability. It is the current research focus to obtain multifunctional solid catalysts with a controlled spatial arrangement of a high-density yet continuous range of different active sites for one-pot heterogeneous tandem reactions, yet it is still challenging.[2]

Metal–organic frameworks (MOFs) are a class of crystalline micro–mesoporous hybrid materials which have already shown a variety of applications.[3] Their inherent high specific surface area and uniform but tunable cavities make MOFs promising heterogeneous catalysts.[4] Since the constituent, topology and surface functionality of MOFs can be readily tuned by varying the metal ions or the bridging organic linkers, MOFs can be an interesting platform to engineer molecular solids for multifunctional catalysis.[5] By adopting this strategy, bi/multi-functionalizations on MOFs have been achieved to catalyze one-pot tandem reactions.[6] However, almost all of the investigated tandem catalytic reactions can only take effect at elevated temperature. Photocatalysis is a unique heterogeneous catalysis, which can make use of solar light as the energy source to achieve organic transformations under mild conditions.[7] Previous studies have revealed that MOFs can be promising photocatalysts for a variety of redox reactions, such as $CO_2$ reduction, water reduction and photooxidation.[8] The coupling of the current MOF-based catalysis with photocatalysis over multi-functional MOFs to achieve some tandem reactions under mild conditions would be appealing, yet this field is almost unexplored. Until recently, Matsuoka *et al.* reported the one pot reaction between benzyl alcohol and malononitrile to synthesize benzylidene malononitrile over $NH_2$-UiO-66(Zr) *via* a coupled photooxidation and Knoevenagel condensation. Unfortunately, the reaction can only be achieved upon UV irradiation and when heated.[6f] Unlike UV light responsive Zr-containing MOFs, all the Fe-based MOF materials already reported show intensive light absorption in the visible light region due to the existence of extensive iron oxo-clusters, which enable them to make effective utilization of solar energy. Moreover, iron is

---

*Research Institute of Photocatalysis, State Key Laboratory of Photocatalysis on Energy and Environment, College of Chemistry, Fuzhou University, Fuzhou 350002, People's Republic of China. E-mail: zhaohuili1969@yahoo.com*

† Electronic supplementary information (ESI) available: Experimental details; characterizations; figures of XRD, IR, BET and UV-vis; other catalytic reaction data. See DOI: 10.1039/c4cy01464b

an earth-abundant metal, which makes it extremely appealing for the application of Fe-containing MOFs in visible-light-induced photocatalysis coupled one-pot tandem reactions.

In this manuscript, we reported a one-pot tandem photo-oxidation/Knoevenagel condensation between benzyl alcohols and active methylene compounds over visible light irradiated $NH_2$-MIL-101(Fe) at room temperature. In addition to acting as a photocatalyst for the oxidation of aromatic alcohols to aldehydes, $NH_2$-MIL-101(Fe) acts as a base catalyst for Knoevenagel condensation between the as-formed aldehydes and the active methylene compounds. The mechanism for the tandem reaction over $NH_2$-MIL-101(Fe) was proposed. This study highlights the great potential of MOFs as multifunctional photocatalysts for one-pot tandem reactions.

## Experimental section

### Preparation

All the reagents and solvents employed were commercially available and used as supplied without further purification. $NH_2$-MIL-101(Fe) was prepared following previously reported procedures.[9] Typically, 0.675 g (2.497 mmol) of $FeCl_3 \cdot 6H_2O$ was dissolved in 7.5 mL of DMF, and a solution of 0.225 g (1.242 mmol) of 2-aminoterephthalic acid in 7.5 mL of DMF was added. After thermal treatment in a stainless steel autoclave for 24 h at 110 °C, the reaction product was recovered by filtration and washed several times with DMF and methanol. Then the obtained solid was finally dried overnight at 60 °C in an oven.

### Characterizations

The as-prepared sample was characterized by X-ray diffraction (XRD) patterns on a D8 Advance X-ray diffractometer (Bruker, Germany) using Cu Kα ($\lambda$ = 1.5406 Å) radiation at a voltage of 40 kV and 40 mA. XRD patterns were scanned over the angular range of 5–25° ($2\theta$) with a step size of 0.02°. The IR experiments were carried out on a Nicolet 670 FT-IR spectrometer. $N_2$ adsorption/desorption experiments were carried out on a Micrometrics ASAP 2020 M volumetric gas sorption instrument. After the sample was degassed in a vacuum at 150 °C for 10 h, the nitrogen adsorption and desorption isotherms were measured at −196 °C. UV-vis diffuse reflectance spectrum (UV-vis DRS) was obtained by a UV-vis spectrophotometer (Varian Cary 500). Barium sulfate ($BaSO_4$) was used as a reference. In the temperature-programmed desorption of $CO_2$ ($CO_2$-TPD; Micromeritics Auto Chem 2920 instrument), the catalyst was pretreated at 150 °C for 2 h. $CO_2$ was adsorbed at 40 °C for 1 h. The sample was, then, flushed for 1 h to remove physical adsorbed $CO_2$. The TPD was conducted from 40 °C to 250 °C at a heating rate of 10 °C $min^{-1}$. The sample was then kept at 250 °C for 2 min.

### Catalytic reactions

The photocatalytic oxidation of benzyl alcohol to benzyl aldehyde was performed as follows. In a typical process, a mixture of benzyl alcohol (0.1 mmol) and trifluorotoluene/acetonitrile (B/A, 10 : 1) (3.0 mL) saturated with $O_2$ was transferred into a 10 mL Schlenk tube containing 20 mg of catalyst. The suspension was irradiated with a 300 W Xe arc lamp (Beijing Perfectlight, PLS-SXE300c) with a UV cutoff filter ($\lambda \geq 420$ nm). For the one-pot tandem reactions, a mixture of aromatic alcohol (0.1 mmol) and active methylene compounds (0.3 mmol) were reacted in B/A (10 : 1) (3.0 mL) saturated with $O_2$. After the reaction, the reaction mixture was filtered through a porous membrane (20 μm in diameter) and the products were determined by GC (Shimadzu GC-2014) equipped with a flame ionization detector using a HP-5 capillary column.

## Results and discussion

$NH_2$-MIL-101(Fe) was synthesized using 2-aminoterephthalic acid ($H_2$ATA) as organic linker according to the procedures reported previously.[9] The XRD patterns and FT-IR spectra of the as-obtained product indicate that pure phase of $NH_2$-MIL-101(Fe) have been obtained (Fig. S1 and S2†). The $N_2$ adsorption/desorption analysis of the as-obtained $NH_2$-MIL-101(Fe) reveals the BET specific surface area to be 2476 $m^2$ $g^{-1}$, comparable to that reported previously (2436 $m^2$ $g^{-1}$) (Fig. S3†).[9b] The UV-vis spectrum of the as-prepared $NH_2$-MIL-101(Fe) shows the absorption edge extending to around 750 nm, in agreement with its brown color (Fig. S4†).

Inspired by a previous report that photocatalytic oxidation of benzyl alcohol to aldehyde can be achieved over visible light irradiated $NH_2$-UiO-66(Zr),[10] we first investigated the visible-light-induced photocatalytic oxidation of benzyl alcohol over $NH_2$-MIL-101(Fe). Like that over $NH_2$-UiO-66(Zr), benzyl alcohol can also be oxidized to benzyl aldehyde over irradiated $NH_2$-MIL-101(Fe) and the reaction medium played an important role in this reaction (Table S1†). Among all the solvents investigated, a mixed solvent containing benzotrifluoride and acetonitrile (B/A) in a 10 : 1 ratio gave the best performance by showing the highest conversion of benzyl alcohol at 39% and a selectivity to benzyl aldehyde at 95% after irradiation for 40 h (Table S1,† entry 4). Control experiments in the absence of $NH_2$-MIL-101(Fe) or without light irradiation did not give any detectable product, indicating that the transformation of benzyl alcohol to benzyl aldehyde was truly induced by the photocatalysis over $NH_2$-MIL-101(Fe) (Table S1,† entry 5 and 6).

Knoevenagel condensation between an active methylene compound and a carbonyl group (C═O) is a useful C–C bond coupling reaction for the preparation of several important chemical intermediates.[11] Previous results have shown that $NH_2$-MIL-101(Fe) can act as a Brønsted base to catalyze the Knoevenagel reaction between benzyl aldehyde and malononitrile due to the existence of the amine functionality.[12] We wondered whether it is possible to couple the photocatalytic oxidation of benzyl alcohol to benzyl aldehyde with the Knoevenagel condensation between benzyl aldehyde and malononitrile over $NH_2$-MIL-101(Fe) in a one-pot reaction. Therefore the reaction between benzyl alcohol and malononitrile in B/A (10 : 1), the best reaction medium observed on the photo-oxidation of benzyl alcohol, was investigated over visible light irradiated $NH_2$-MIL-101(Fe). To our anticipation, the reaction between benzyl alcohol with malononitrile over $NH_2$-MIL-101(Fe) gave benzylidene malononitrile as the main product, indicating the successful coupling of photo-oxidation with the Knoevenagel condensation in a one pot tandem reaction. As shown in Fig. 1, the formation of benzylidene malononitrile increased with the irradiation time and after irradiation for 40 h, the conversion of benzyl alcohol reached 88% with the yield of benzylidene malononitrile at 72% (Fig. 1a and Table 1, entry 1). In addition to benzyl aldehyde (5%) and benzylidene malononitrile, β-hydroxyl benzalmalononitrile with a yield of 9% was also detected. It is interesting to observe that the conversion of benzyl alcohol in the multi-component reaction is higher than that observed over photo-oxidation alone (39%, Table S1,† entry 4), indicating that the removal of the intermediate (benzyl aldehyde) is beneficial to the photo-oxidation reaction. Control experiments in absence of either $NH_2$-MIL-101(Fe) or visible light irradiation under otherwise similar conditions gave almost negligible products, indicating that the formation of benzylidene malononitrile was truly induced by the irradiated $NH_2$-MIL-101(Fe) (Table 1, entry 2 and 3). The heterogeneous nature of this reaction was confirmed by the filtrate reaction. No further reaction occurred in the filtrate after the solid catalyst was removed from the reaction system after 12 h irradiation (Fig. 1b). The recycling of the photocatalyst for three runs showed no obvious decrease of the photocatalytic activity (Fig. 2). Besides this, the XRD, IR and $N_2$ adsorption/desorption isotherms of the photocatalyst after the reaction did not show much change (Fig. S5–S7†). All these suggest that $NH_2$-MIL-101(Fe) is stable and reusable during the reaction.

Having established that $NH_2$-MIL-101(Fe) can catalyze the one-pot reaction between benzyl alcohol and malononitrile, we extend the study to various substrates, including different alcohols and other active methylene compounds. First, a series of substituted aromatic alcohols were selected as the substrates and reacted with malononitrile. Although the transformations of all the aromatic alcohol derivatives to the corresponding benzylidene malononitriles proceeded under the reaction conditions, the different substituents on the phenyl ring influenced the conversion ratio and suggested the existence of an electronic effect. As compared with bare benzyl alcohol, aromatic alcohols with electron-withdrawing substituents like $-NO_2$ showed a significantly decreased conversion ratio (24%, Table 1, entry 4), while aromatic alcohols with *para*-substituted electron donating groups like $-CH_3$ and $-OCH_3$ exhibited a slightly increased conversion ratio (90–93%, Table 1, entry 5 and 6). The existence of the steric hindrance on this reaction was also observed since aromatic alcohols with a methyl group ($-CH_3$) substituted at different positions of phenyl ring showed reaction rates in the order of *meta*- < *ortho*- < *para*-substituted (Table 1, entry 6–8). The reaction between the benzyl alcohol with other organics containing active methylene groups, like ethyl cyanoacetate or diethyl malonate, also occurred over $NH_2$-MIL-101(Fe) under visible light irradiations, but the performance for different substrates varied. For the reaction between ethyl cyanoacetate and benzyl alcohol, the reaction proceeded efficiently with 83% of benzyl alcohol converted in 40 h, and a relatively high yield of 66% to ethyl (benzylidene)cyanoacetate was achieved (Table 1, entry 9). On the contrary, the reaction between benzyl alcohol and diethyl malonate did not proceed smoothly. A low conversion of benzyl alcohol (18%) with an even lower yield of diethyl benzylidene malonate (2.7%) was observed (Table 1, entry 10). The different reactivity of the methylene compounds can be well explained in terms of their different acidity, which decreases in the order of malononitrile ($pK_a$ = 11.1) > ethyl cyanoacetate ($pK_a$ = 13.1) > diethyl malonate ($pK_a$ = 16.4).[13] Since the first step of the Knoevenagel condensation involves the deprotonation of the active methylene group, the higher $pK_a$ value of the methylene group in diethyl malonate (16.4) indicates that the deprotonation of diethyl malonate is difficult, which leads to the low efficiency of the formation of diethyl benzylidene malonate *via* Knoevenagel condensation between benzyl aldehyde and diethyl malonate.[14]

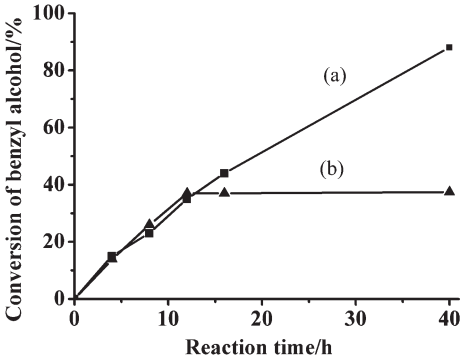

**Fig. 1** Conversion ratio of benzyl alcohol as a function of irradiation time in a one-pot tandem reaction over: (a) $NH_2$-MIL-101(Fe); and (b) the reaction system after $NH_2$-MIL-101(Fe) was removed after irradiated for 12 h.

The one-pot reaction between aromatic alcohols and active methylene compounds over $NH_2$-MIL-101(Fe) *via* tandem photo-oxidation/Knoevenagel condensation can be well illustrated in the following Scheme 1. First, the aromatic alcohol was photocatalytically oxidized to aldehyde over irradiated $NH_2$-MIL-101(Fe). It is believed that the organic linker ATA in $NH_2$-MIL-101(Fe) acts as an antenna to absorb visible light. Upon irradiation, the excited ligand ATA can transfer electrons to the Fe-oxo clusters, and $Fe^{3+}$ in the Fe–O clusters is reduced to $Fe^{2+}$, which can reduce $O_2$ to form $O_2^{\bullet-}$ radical (step a). In the meantime, the organic substrates adsorbed on the surface of the MOF material can donate an electron to form the carbonium ions (step b), which can further react with the as-formed $O_2^{\bullet-}$ radicals to form the aromatic aldehydes (step c). The confinement effect of the nanometer-sized cavities in MOF material helps to stabilize the as-formed $O_2^{\bullet-}$ radical and the reactive intermediates. Such a photo-oxidation

**Table 1** Reaction between substituted aromatic alcohols and active methylene compounds over $NH_2$-MIL-101(Fe)

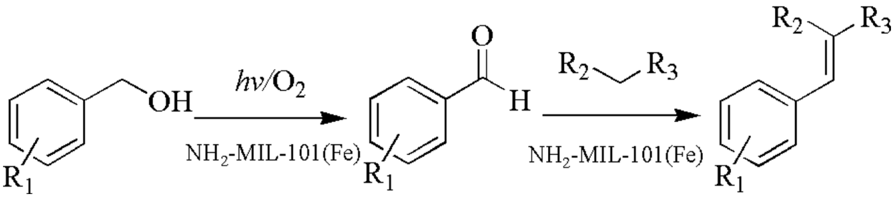

| | Substrates | | | Yield (%) | |
|---|---|---|---|---|---|
| Entry | 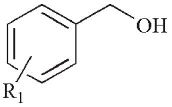 $R_1$= |  | Conv. of alcohol (%) | 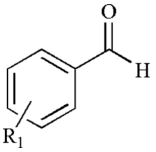 | 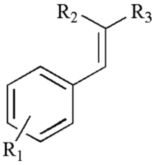 |
| 1 | –H | $R_2,R_3$ = –CN | 88 | 5 | 72 |
| 2[a] | –H | $R_2,R_3$ = –CN | 0.9 | —[c] | — |
| 3[b] | –H | $R_2,R_3$ = –CN | 0.8 | — | — |
| 4 | $-NO_2$ | $R_2,R_3$ = –CN | 24 | 3.7 | 20 |
| 5 | *p*-$OCH_3$ | $R_2,R_3$ = –CN | 93 | 8 | 76 |
| 6 | *p*-$CH_3$ | $R_2,R_3$ = –CN | 90 | 5.5 | 76 |
| 7 | *m*-$CH_3$ | $R_2,R_3$ = –CN | 80 | 7 | 63 |
| 8 | *o*-$CH_3$ | $R_2,R_3$ = –CN | 82 | 6.1 | 66 |
| 9 | –H | $R_2$ = –CN<br>$R_3$ = –COOEt | 83 | 5.4 | 66 |
| 10 | –H | $R_2,R_3$ = –COOEt | 18 | 12 | 2.7 |

Reaction conditions: aromatic alcohols (0.1 mmol), methylene compounds (0.3 mmol), B/A (10 : 1) (3 mL), $NH_2$-MIL-101(Fe) (20 mg), $O_2$ (1 atm), light irradiation ($\lambda \geq 420$ nm), 40 h.[a] Without visible light irradiation. [b] No catalyst. [c] "—" refers to no products, or negligible products were detected.

mechanism has already been demonstrated previously over irradiated $NH_2$-UiO-66(Zr).[10] Due to the existence of the basic $-NH_2$ site in $NH_2$-MIL-101(Fe), the as-formed aromatic aldehydes can further react with active methylene compounds *via* a Knoevenagel condensation. The first step in this process involves the deprotonation of the active methylene group under the assistance of the basic $-NH_2$ site in $NH_2$-MIL-101(Fe) to form a carbonanion (step i). The as-formed carbon anion can make a nucleophilic attack on the carbonyl carbon atoms of the aromatic aldehydes (step ii). The as-formed intermediate can take up one proton from the catalyst to form the β-hydroxyl compound, and the catalyst is regenerated (step iii). Finally, the β-hydroxyl compound can eliminate one molecule of water to make an α,β-unsaturated compound (step iv).

The reaction between benzyl alcohol and malononitrile over other amine-functionalized photocatalytic active MOFs like $NH_2$-MIL-125(Ti) and $NH_2$-UiO-66(Zr) under visible light irradiations was also investigated and the results are shown in Table 2. Although the reaction between benzyl alcohol and malononitrile also led to the formation of benzylidene malononitrile over all three MOFs, both the conversion ratio of the benzyl alcohol and the yield of benzylidene malononitrile varied significantly among these MOFs. The yield of benzylidene malononitrile was much lower over

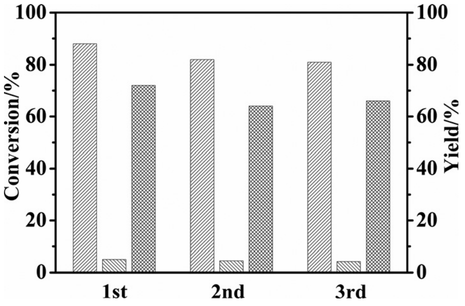

**Fig. 2** Conversion of benzyl alcohol (▨) and yields to benzaldehyde (▧), benzylidene malononitrile (▩) in the one-pot tandem reaction over $NH_2$-MIL-101(Fe) for recycling use.

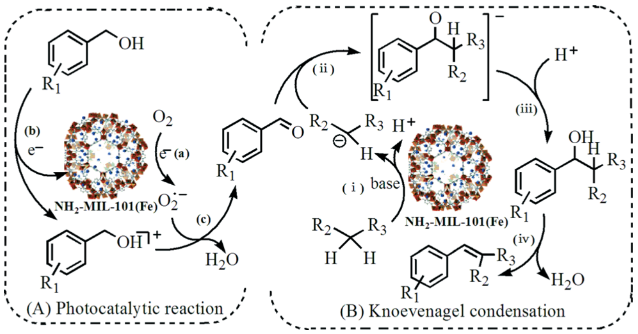

**Scheme 1** Proposed mechanism for one-pot tandem photocatalytic oxidation/Knoevenagel condensation over bi-functional $NH_2$-MIL-101(Fe).

**Table 2** One-pot tandem reaction over different MOFs[a]

| Entry | Catalyst | Conv. of alcohol (%) | Yield (%) | |
|---|---|---|---|---|
| | | | Benzyl aldehyde | Benzylidene malononitrile |
| 1 | $NH_2$-MIL-101(Fe) | 88 | 5 | 72 |
| 2 | $NH_2$-UiO-66(Zr) | 38 | 29 | 4.6 |
| 3 | $NH_2$-MIL-125(Ti) | 47 | 39 | 3.3 |

[a] Reaction conditions: benzyl alcohol (0.1 mmol), malononitrile (0.3 mmol), B/A (10 : 1) (3 mL), MOFs (20 mg), $O_2$ (1 atm), light irradiation ($\lambda \geq 420$ nm), 40 h.

irradiated $NH_2$-UiO-66(Zr) (4.6%) and $NH_2$-MIL-125(Ti) (3.3%) under otherwise similar reaction conditions as compared to that over $NH_2$-MIL-101(Fe) (72%). However, the photocatalytic oxidation of benzyl alcohol to form benzyl aldehyde over $NH_2$-UiO-66(Zr) (28%) and $NH_2$-MIL-125(Ti) (37%) was comparable to that over irradiated $NH_2$-MIL-101(Fe) (39%) (Table S2†). This indicates that the lower efficiency of the one-pot photo-oxidation/Knoevenagel condensation over $NH_2$-UiO-66(Zr) and $NH_2$-MIL-125(Ti) was induced by their lower efficiency in the Knoevenagel condensation, instead of the lower activity for the photo-oxidation. This assumption is confirmed by the control Knoevenagel reaction between benzaldehyde and malononitrile under otherwise similar conditions, which shows a similar activity order of $NH_2$-MIL-101(Fe) > $NH_2$-Uio-66(Zr) > $NH_2$-MIL-125(Ti) (Fig. S8†).

Based on the proposed mechanism, the efficiency of Knoevenagel condensation is mainly dependent on the deprotonation of the active methylene group. Therefore, the strength of the basic site in different MOF materials should play an important role in the Knoevenagel reaction. To explore the basic characteristic of the above three MOF materials, their $CO_2$-TPD profiles were investigated and the results are shown in Fig. 3. TPD is a very useful technique for characterizing chemically bonded surfaces or adsorbed species and the $CO_2$-TPD profile has been used extensively in determining the basic strength of the catalyst.[15] As shown in Fig. 3(a), the $CO_2$-TPD profile of $NH_2$-MIL-101(Fe) shows three peaks at $T_{max}$ of 118 °C, 217 °C and 240 °C. The desorption peak occuring at 217 °C can be ascribed to desorption of $CO_2$ adsorbed on the basic –$NH_2$ site. As compared with the $CO_2$-TPD file of $NH_2$-MIL-101(Fe), those of $NH_2$-UiO-66(Zr) and $NH_2$-MIL-125(Ti) also show big desorption peaks, corresponding to desorption of $CO_2$ adsorbed on a basic site (–$NH_2$). However, the desorption peak of $NH_2$-UiO-66(Zr) occurs at 214 °C (Fig. 3(b)), while that of $NH_2$-MIL-125(Ti) occurs at 192 °C (Fig. 3(c)). Since the basic strength of the catalyst is correlated with the desorption temperature in the $CO_2$-TPD profile, the lower desorption temperature observed over $NH_2$-UiO-66(Zr) and $NH_2$-MIL-125(Ti) indicate that the strength of the basic sites in these two MOFs are not as strong as that in $NH_2$-MIL-101(Fe). Therefore, the Knoevenagel condensation over $NH_2$-UiO-66(Zr) and $NH_2$-MIL-125(Ti) is not as efficient as that over $NH_2$-MIL-101(Fe).

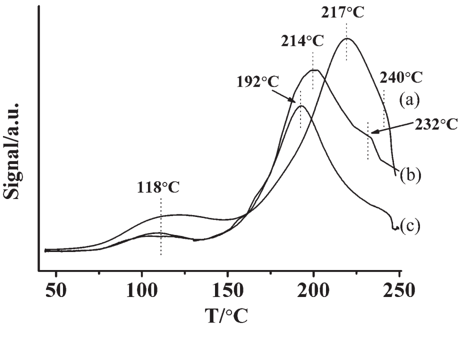

**Fig. 3** $CO_2$-TPD profiles of $CO_2$ adsorbed MOF materials: (a) $NH_2$-MIL-101(Fe); (b) $NH_2$-UiO-66(Zr); (c) $NH_2$-MIL-125(Ti).

## Conclusion

In summary, $NH_2$-MIL-101(Fe) can catalyze the one-pot reaction between aromatic alcohols and active methylene compounds under visible light and at room temperature. $NH_2$-MIL-101(Fe) acts as a photocatalyst for oxidation of aromatic alcohols to aldehydes as well as a base catalyst for Knoevenagel condensation between the as-formed aromatic aldehydes and the active methylene compounds. The efficiency of the tandem reaction is significantly influenced by the strength of the basic sites in the MOF materials. We believe that the present study will stimulate intensive research in developing MOF-based multifunctional photocatalysts for one-pot tandem reactions. Considering the versatile structures of MOF materials and their facile modulations, it is believed that more and more multifunctional MOF-based photocatalysts for one-pot tandem reaction can be obtained.

## Acknowledgements

This work was supported by NSFC (21273035), 973 Programs (2014CB239303) and Specialized Research Fund for the Doctoral Program of Higher Education (20123514110002). Z. Li thanks the Award Program for Minjiang Scholar Professorship for financial support.

## References

1 (*a*) J. M. Lee, Y. Na, H. Han and S. Chang, *Chem. Soc. Rev.*, 2004, 33, 302; (*b*) J.-C. Wasilke, S. J. Obrey, R. T. Baker and G. C. Bazan, *Chem. Rev.*, 2005, **105**, 1001.
2 (*a*) J. M. Notestein and A. Katz, *Chem. – Eur. J.*, 2006, **12**, 3954; (*b*) Y. Yang, X. Liu, X. Li, J. Zhao, S. Bai, J. Liu and

Q. Yang, *Angew. Chem., Int. Ed.*, 2012, **51**, 9164; (*c*) C. Yu and J. He, *Chem. Commun.*, 2012, **48**, 4933.

3 (*a*) P. Horcajada, R. Gref, T. Baati, P. K. Allan, G. Maurin, P. Couvreur, G. Férey, R. E. Morris and C. Serre, *Chem. Rev.*, 2012, **112**, 1232; (*b*) T. R. Cook, Y. R. Zheng and P. J. Stang, *Chem. Rev.*, 2013, **113**, 734; (*c*) J. R. Li, J. Sculley and H. C. Zhou, *Chem. Rev.*, 2012, **112**, 869; (*d*) B. Chen, S. Xiang and G. Qian, *Acc. Chem. Res.*, 2010, **43**, 1115; (*e*) K. Sumida, D. L. Rogow, J. A. Mason, T. M. McDonald, E. D. Bloch, Z. R. Herm, T.-H. Bae and J. R. Long, *Chem. Rev.*, 2012, **112**, 724; (*f*) J. Lee, O. K. Farha, J. Roberts, K. A. Scheidt, S. T. Nguyen and J. T. Hupp, *Chem. Soc. Rev.*, 2009, **38**, 1450.

4 (*a*) A. Corma, H. García and F. X. L. I. Xamena, *Chem. Rev.*, 2010, **110**, 4606; (*b*) W. M. Xuan, C. F. Zhu, Y. Liu and Y. Cui, *Chem. Soc. Rev.*, 2012, **41**, 1677; (*c*) A. Dhakshinamoorthy, M. Opanasenko, J. Čejka and H. Garcia, *Catal. Sci. Technol.*, 2013, **3**, 2509; (*d*) W.-Y. Gao, M. Chrzanowski and S. Q. Ma, *Chem. Soc. Rev.*, 2014, **43**, 5841; (*e*) K. G. M. Laurier, F. Vermoortele, R. Ameloot, D. E. D. Vos, J. Hofkens and M. B. J. Roeffae, *J. Am. Chem. Soc.*, 2013, **135**, 14488; (*f*) A. Dhakshinamoorthy, M. Alvaro and H. Garcia, *Catal. Sci. Technol.*, 2011, **1**, 856; (*g*) D. K. Wang, R. K. Huang, W. J. Liu, D. R. Sun and Z. H. Li, *ACS Catal.*, 2014, **4**, 4254.

5 (*a*) C. Wang, D. Liu and W. B. Lin, *J. Am. Chem. Soc.*, 2013, **135**, 13222; (*b*) J. Gascon, A. Corma, F. Kapteijn and F. X. L. I. Xamena, *ACS Catal.*, 2011, **1**, 1734; (*c*) T. Truong, C. K. Nguyen, T. V. Tran, T. T. Nguyen and N. T. S. Phan, *Catal. Sci. Technol.*, 2014, **4**, 1276.

6 (*a*) M. Yoon, R. Srirambalaji and K. Kim, *Chem. Rev.*, 2012, **112**, 1196; (*b*) R.-Q. Zou, H. Sakurai and Q. Xu, *Angew. Chem., Int. Ed.*, 2006, **45**, 2542; (*c*) R. Srirambalaji, S. Hong, R. Natarajan, M. Yoon, R. Hota, Y. Kim, Y. H. Ko and K. Kim, *Chem. Commun.*, 2012, **48**, 11650; (*d*) M. Pintado-Sierra, A. M. Rasero-Almansa, A. Corma, M. Iglesias and F. Sánchez, *J. Catal.*, 2013, **299**, 137; (*e*) F. Vermoortele, R. Ameloot, A. Vimont, C. Serre and D. D. Vos, *Chem. Commun.*, 2011, **47**, 1521; (*f*) T. Toyao, M. Saito, Y. Horiuchi and M. Matsuoka, *Catal. Sci. Technol.*, 2014, **4**, 625; (*g*) B. Li, Y. Zhang, D. Ma, L. Li, G. Li, G. Li, Z. Shi and S. Feng, *Chem. Commun.*, 2012, **48**, 6151; (*h*) P. Y. Wu, C. He, J. Wang, X. J. Peng, X. Z. Li, Y. L. An and C. Y. Duan, *J. Am. Chem. Soc.*, 2012, **134**, 14991.

7 X. J. Lang, X. D. Chen and J. C. Zhao, *Chem. Soc. Rev.*, 2014, **43**, 473.

8 (*a*) Y. H. Fu, D. R. Sun, Y. J. Chen, R. K. Huang, Z. X. Ding, X. Z. Fu and Z. H. Li, *Angew. Chem., Int. Ed.*, 2012, **51**, 3364; (*b*) D. R. Sun, Y. H. Fu, W. J. Liu, L. Ye, D. K. Wang, L. Yang, X. Z. Fu and Z. H. Li, *Chem. – Eur. J.*, 2013, **19**, 14279; (*c*) Y. Horiuchi, T. Toyao, M. Saito, K. Mochizuki, M. Iwata, H. Higashimura, M. Anpo and M. Matsuoka, *J. Phys. Chem. C*, 2012, **116**, 20848; (*d*) C. Wang, Z. G. Xie, K. E. deKrafft and W. B. Lin, *J. Am. Chem. Soc.*, 2011, **133**, 13445; (*e*) M.-H. Xie, X.-L. Yang, C. Zou and C.-D. Wu, *Inorg. Chem.*, 2011, **50**, 5318.

9 (*a*) S. Bauer, C. Serre, T. Devic, P. Horcajada, J. Marrot, G. Férey and N. Stock, *Inorg. Chem.*, 2008, **47**, 7568; (*b*) M. Savonnet, E. Kockrick, A. Camarata, D. Bazer-Bachi, N. Bats, V. Lecocq, C. Pinel and D. Farrusseng, *New J. Chem.*, 2011, **35**, 1892.

10 J. L. Long, S. B. Wang, Z. X. Ding, S. C. Wang, Y. G. Zhou, L. Huang and X. X. Wang, *Chem. Commun.*, 2012, **48**, 11656.

11 (*a*) M. J. Climent, A. Corma and S. Iborra, *Chem. Rev.*, 2011, **111**, 1072; (*b*) S. Shylesh, A. Wagner, A. Seifert, S. Ernst and W. R. Thiel, *Chem. – Eur. J.*, 2009, **15**, 7052.

12 M. Hartmann and M. Fischer, *Microporous Mesoporous Mater.*, 2012, **164**, 38.

13 (*a*) W. N. Olmstead and F. G. Bordwell, *J. Org. Chem.*, 1980, **45**, 3299; (*b*) F. G. Bordwell and H. E. Fried, *J. Org. Chem.*, 1981, **46**, 4328; (*c*) B. R. Gelin and M. Karplus, *J. Am. Chem. Soc.*, 1975, **97**, 6996.

14 Y. Yang, H.-F. Yao, F.-G. Xi and E.-Q. Gao, *J. Mol. Catal. A: Chem.*, 2014, **390**, 198.

15 L. K. Ono and B. R. Cuenya, *J. Phys. Chem. C*, 2008, **112**, 18543.